Environmental Research 200 (2021) 111414

Contents lists available at ScienceDirect

Environmental Research

journal homepage: www.elsevier.com/locate/envres

A sustainable green synthesis of functionalized biocompatible carbon quantum dots from *Aloe barbadensis* Miller and its multifunctional applications

Jalaja Prasad Malavika [a], Chellappan Shobana [a,*], Murugesan Ragupathi [b], Ponnuchamy Kumar [c], Yun Sung Lee [d], Muthusamy Govarthanan [e], Ramakrishnan Kalai Selvan [b,**]

[a] Department of Zoology, Kongunadu Arts and Science College (Autonomous), G. N. Mills, Coimbatore, 641 029, Tamil Nadu, India
[b] Department of Physics, Bharathiar University, Coimbatore, 641 046, Tamil Nadu, India
[c] Department of Animal Health and Management, Alagappa University, Karaikudi, 630 003, India
[d] Faculty of Applied Chemical Engineering, Chonnam National University, Gwangju, 500-757, South Korea
[e] Department of Environmental Engineering, Kyungpook National University, Daegu, 41566, Republic of Korea

ARTICLE INFO

Keywords:
Green synthesis
Carbon quantum dots
Photocatalyst
MCF-7 human breast cancer cell line
Fluorescent probes

ABSTRACT:

Herein, we demonstrated a sustainable green approach for the preparation of fluorescent biocompatible carbon quantum dots by microwave-assisted reflux synthesis from *Aloe barbadensis* Miller (Aloe vera) extract. The Transmission Electron Microscopic images reveal that the as-prepared CQDs are spherical with less than 5 nm in size. The CQDs are amorphous, showed an excitation-independent behaviour, emitted blue fluorescence and have a fluorescence quantum yield of 31%. The presence of –OH groups contributed to the blue emission and helped CQDs to disperse uniformly in an aqueous solution. The prepared CQDs were employed as a photocatalyst for the environmental remediation to degrade the anionic dye, eosin yellow under visible light irradiation. The results showed that the CQDs exhibited excellent photocatalytic efficiency of 98.55% within 80 min and a 100% efficiency within 100 min. Further, the cytotoxic properties of as-prepared CQDs are investigated in the MCF-7 breast cancer cell line using MTT assay. The results demonstrated a notable reduction in cell viability in a dose-subjected manner, and the cell viability decreased to 50% (IC_{50}) at a concentration of 52.2 ± 1.35 μg/mL. Furthermore, cellular internalization of CQDs in breast cancer cells is studied. As expected, CQDs are found to internalize by the cancer cells with blue emission as revealed by fluorescence microscope. In the end, CQDs in human breast cancer cells demonstrate the anti-proliferative effect and are found to be an impressive fluorescent probe for live-cell imaging, paving a path for its potential biomedical applications.

1. Introduction

Carbon quantum dots (CQDs) have received huge attention in recent years due to their outstanding properties for the replacement of conventional quantum dots in diverse applications (Semeniuk et al., 2019). CQDs belong to novel zero-dimensional carbon-based nanomaterials, either a crystalline or amorphous structure, having sp^2 hybridization in most cases followed by sp^3 hybridization (Wang et al., 2019; Molaei et al., 2019). Interestingly, carbon quantum dots exhibit exceptional optical and fluorescence characteristics, high aqueous solubility and are rich in emission quantum yield, simple surface functionalization and high thermal as well as optical photostability that entrusts them for use in various cutting edge applications especially in the area of energy, environment and health care sectors (Sagbas and Sahiner, 2019).

By considering the fascinating optical and electronic properties including effective absorbance of solar light, tunable photoluminescence (PL), infrared-responsive up-converted photoluminescence (UCPL) and unique photoinduced electron transfer, the CQDs are potentially considered as an efficient photocatalyst (Wang et al., 2017b). Recent studies elucidated that the photocatalytic process is one of the most

* Corresponding author.
** Corresponding author.
E-mail addresses: cshobana_zo@kongunaducollege.ac.in (C. Shobana), selvankram@buc.edu.in (R.K. Selvan).

https://doi.org/10.1016/j.envres.2021.111414
Received 7 January 2021; Received in revised form 6 May 2021; Accepted 18 May 2021
Available online 27 May 2021

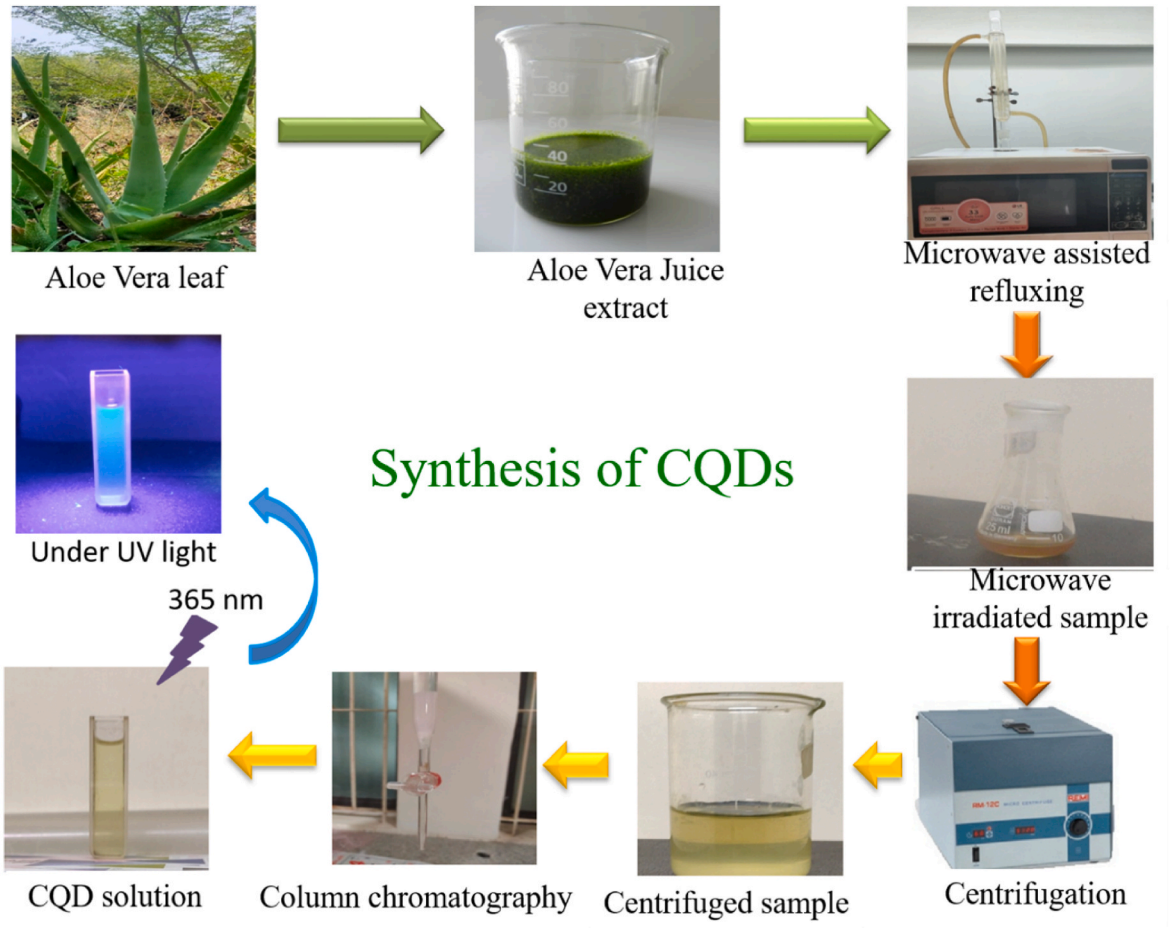

Fig. 1. Schematic illustration of the preparation of CQDs from Aloe vera leaf extract.

energy-efficient technique to remove the pollutants and dyes from the water and wastewater through advanced oxidation processes (AOP) when compared with the other techniques including biodegradation, adsorption, coagulation, membrane phase, etc. (Pirsaheb et al., 2018). It is well known that dyes are the major pollutant or hazardous material available in untreated effluents (Karthik et al., 2016). Further, the coloured dyes are resistant to biodegradation and can hardly be removed from effluents using conventional wastewater treatments because of their complicated chemical compositions.

Eosin yellow is a common textile dye that belongs to the fluorescence class and being widely used for staining purposes. But, its toxicological information listed it as carcinogenic, which can cause severe skin and eye irritation and hurt vital organs (Anirudhan et al., 2015; Mittal et al., 2013). The (photo) degradation process of EY is difficult since this dye is highly light-sensitive and has a high pH dependency when compared with the other cationic dyes (Majek et al., 2014; Zheng et al., 2007). Many of the existing photocatalytic systems suffer from low sunlight utilization and high recombination rates of photoinduced charge carriers, which limits the overall quantum efficiency and practicality of photocatalysis. Hence in the present work, the CQDs are employed as a photocatalytic agent for the degradation of EY, without the combination of any semiconductor nanomaterial or heteroatom doping.

Apart from this, the other properties of CQDs such as superiority in aqueous solubility, chemical stability, low cytotoxicity and its rich in emission quantum yield that entrusts them for use in biomedical applications especially in *in-vivo* and *in vitro* bio-imaging (Jhonsi et al., 2018). It has been found that CQDs have anti-proliferative, cytotoxic and apoptosis effect on cancer cells, which paves a path for cancer treatment with better potential (Arkan et al., 2018). The ability of CQDs to exhibit anticancer effect has been attributed to different factors, and a unified underlying molecular mechanism is not yet elucidated (Li et al., 2014). But the CQDs can interact with the cancer cells resulting in the formation of Reactive Oxygen Species (ROS), which can kill cancer cells. Especially, carbon quantum dots derived from biomasses have been widely used in *in-vivo* and *in-vitro* bio-imaging of MCF-7 (Arkan et al., 2018; Arumugham et al., 2020; Yao et al., 2018) and other cancer cell lines (Alam et al., 2015).

The conventional chemical methods make use of toxic and harsh chemical additives for the synthesis of CQDs that provide risks to the biological environment. Therefore, green synthesis is attracting massive attention in recent years, where plant-based materials are used as the source to synthesize CQDs. As well, this method is sustainable and eco-friendly by minimizing wastes and reducing pollution. Similarly, the produced CQDs have high biocompatibility since the reducing agents and stabilizing agents, are naturally present in the biomasses (Singh et al., 2018). It has been reported that the CQDs synthesized from walnut oil (Arkan et al., 2018), and ginsenoside Re (Yao et al., 2018) were found to have anticancer property against MCF-7 human breast cancer cell lines. Overall, the biomass precursors for the preparation of CQDs were found to exhibit multifunctional applications in both environmental and biological regime.

In this line, the *Aloe barbadensis* Miller (Aloe vera) is preferred for the synthesis of biocompatible *in-situ* functionalized CQDs as the green precursor. Aloe vera is a hardy, perennial, tropical, drought-resistant and succulent plant of the Liliaceae family. It is used in several cultures, in different medicinal fields like Ayurveda, Siddha, Unani and homoeopathy. Clinical evaluations indicated the presence of 75 potentially active constituents, which are pharmacologically active

ingredients in the rind and gel of the Aloe vera leaves (Nandal et al., 2012). As well, the components in Aloe vera inhibited the proliferation of human breast and cervical cancer cell lines (Hussain et al., 2015) and hepatocellular cancer cell lines (Shalabi et al., 2015). These results showed the high possibility of CQDs synthesized from Aloe vera leaf extract possessing anticancer property. Previously, Sarkar et al. (2017) and Xu et al. (2015) have developed high fluorescent CQDs from Aloe vera leaf gel by time-consuming carbonization and hydrothermal methods, respectively. On the other hand, microwave-assisted synthesis is a widely accepted technique for the synthesis of CQDs due to its ability for promoting reactions more energy efficient through creating homogeneous temperature and rapid action compared to the conventional heat conduction methods (Singh et al., 2019).

Therefore, herein simple, single-step and rapid microwave-assisted reflux method is adopted for the synthesis of CQDs from Aloe vera extract without using any reducing agents and studied their physicochemical properties. Further, the synthesized CQDs are utilized for the visible-light-induced degradation of anionic eosin yellow dye. The anticancer activity of as-synthesized CQDs was carried out using an MTT assay against MCF-7 human breast cancer cell lines. Furthermore, the fluorescence microscopy technique is used to detect cellular morphology and to study the bio-imaging potential of CQDs on the cancer cell line.

2. Experimental methods and materials

2.1. Microwave-assisted reflux green synthesis of carbon quantum dots

Fig. 1 shows the schematic representation for the preparation of carbon quantum dots from Aloe vera extract using the m*icrowave-assisted reflux green synthesis method* (Shobana et al., 2018). For the typical synthesis, the healthy and fresh leaves of Aloe vera were collected, washed several times with double-distilled water. The 50 mg of smashed leaf pieces were mixed with 50 ml of double-distilled water. Further, the mixed solution was transferred to a 100 ml round bottom flask and kept in the domestic LG microwave oven with an operating frequency of 2.45 GHz, and output power of 80 W. Top of the microwave oven was equipped with a water-cooled condenser to prevent the loss of Aloe vera extract by evaporation. The reaction proceeds with the continuous 1 min "on" and 30 s "off". Subsequently, it is allowed to cool at room temperature. Finally, the solution was centrifuged at 5000 rpm for 20 min to remove undesired impurities. Further, the CQDs are separated by the silica gel column separation method and followed by dialysis (MW: 12–14 kDa in Milli-Q water). The reaction was repeated at regular intervals of 4, 5, 6, 7 and 8 min. The obtained fluorescence emission under UV light confirmed the formation of CQDs from the biomass (Hasan et al., 2021).

2.2. Characterization techniques

Subsequently, the physicochemical properties of CQDs are measured using UV–visible spectroscopy (JascoV-550), photoluminescence spectroscopy (PL) (Horiba Jobin Yvon Fluoromax-4 spectrofluorometer), X-Ray Diffraction (XRD) (Malvern PANalytical multipurpose diffractometer), Fourier Transform Infrared Spectroscopy (FT-IR) (Shimadzu IFS 66V FTIR) and X-ray Photoelectron Spectroscopy (XPS) (Kratos Analytical, Ultra axis instrument). The morphology and particle size distribution of CQDs are measured by using Transmission Electron Microscopy (TEM) (JEOL JEM 2100 High-Resolution Transmission Electron Microscope (HRTEM)).

2.3. Quantum yield calculations

The fluorescence quantum yield (QY) of CQDs are calculated using the established procedure by Arkan et al. (2018). In this regard, quinine sulphate (in 0.10 M H_2SO_4) was chosen as the reference to determine the QY of CQDs at various concentrations. All the optical emissions were recorded at 360 nm excitation, which should not exceed 0.1 to reduce or avoid internal filter effects. The integrated fluorescence intensity was determined by calculating the area under the photoluminescence curve from 380 to 700 nm. The integrated fluorescence intensity and the absorbance values were used to calculate the QY (equation (1)):

$$\phi = \phi_{std} \left[\frac{I_x}{A_x}\right] \left[\frac{A_R}{I_R}\right] \left[\frac{\eta_x}{\eta_R}\right]^2 \quad (1)$$

Where ϕ refers to quantum yield of CQDs, 'I' is the measured integrated intensity, η is the refractive index and A is the optical absorption. The subscript 'x' and 'R' denotes the CQDs and quinine sulphate samples, respectively.

2.4. Photocatalytic measurements

For the photocatalytic studies (Sabet et al., 2019; Das et al., 2019a), 1.55 mg (in 50 ml of water) of eosin yellow was mixed with 200 μl of CQDs and stirred for 30 min under the dark condition to reach the equilibrium state. Further, the desired amount of mixed solution was subjected to expose the sunlight between 11.00 a.m. and 2.00 p.m. without sealing. The experiments were carried out at the Bharathiar University campus (76.8764° E and 11.0390° N). The samples were collected for every 20-min intervals. Finally, the degradation level of the eosin yellow was studied using a UV–vis spectrometer by measuring the spectra in the wavelength range between 200 and 800 nm.

2.5. Cell viability studies – MTT assay

For cell culture-based studies, MCF-7 human breast cancer cells were procured from National Centre for Cell Science (NCCS), Pune. The obtained cells revived in Dulbecco's Modified Eagle's Medium (DMEM) provided with 10% fetal bovine serum (FBS) and 1% antibiotics (penicillin and streptomycin) in an incubator supplied with 5% CO_2 at 37 °C. The cytotoxic effect of CQDs was analyzed in the MCF-7 human breast cancer cell line. MCF-7 human breast cancer cell lines were cultured with 5% (v/v) fetal bovine serum in 100 U/mL penicillin and 100 mg/mL streptomycin in Dulbecco's modified Eagle medium (DMEM). The medium was replaced within 2–3 days and sub-cultured once the cell population density reached a confluence of 70–80%.

MTT assay was used to evaluate the inhibitory effects of CQDs on the growth of the MCF-7 cell line. Briefly, the cells were suspended at a concentration of 1×10^5 cells/mL in a mixture of DMEM and 10% bovine serum, 100 units/mL of penicillin, and 100 μga/mL of streptomycin. The cell suspension was pipetted into a 96-well plate (100 μL/well) and was allowed to adhere at 37 °C in a humidified incubator containing 5% CO_2. After 24 h of seeding, the cells were treated in different concentrations (0–100 μg/mL) of CQDs dissolved in DMSO. In the end, the medium was replaced by 100 μL of 0.5 mg/mL of MTT in the growth medium after 24 h and was incubated at 37 °C for 3 h. Followed by this, the supernatant was removed carefully, and 100 μL of DMSO was added to each well to dissolve formazan crystals. Then, the absorbance was read at 595 nm using a microliter plate reader to determine the half-maximum inhibitory concentration (IC_{50}) of CQDs.

2.6. In-vitro bio-imaging studies

Briefly, the cells were suspended at a concentration of 1×10^6 cells/mL were seeded onto a 6 well plate and allowed to adhere at 37 °C in a humidified incubator containing 5% CO_2. After 24 h, about 10 μL (10 μg/mL) of CQDs in 1 mL of PBS was added to the cell culture medium followed by incubation for 1 h at 37 °C in a 5% CO_2 environment. After incubation, the cells were imaged under a fluorescence microscope (Accu-Scope EXI-310, USA) at 20 X magnification.

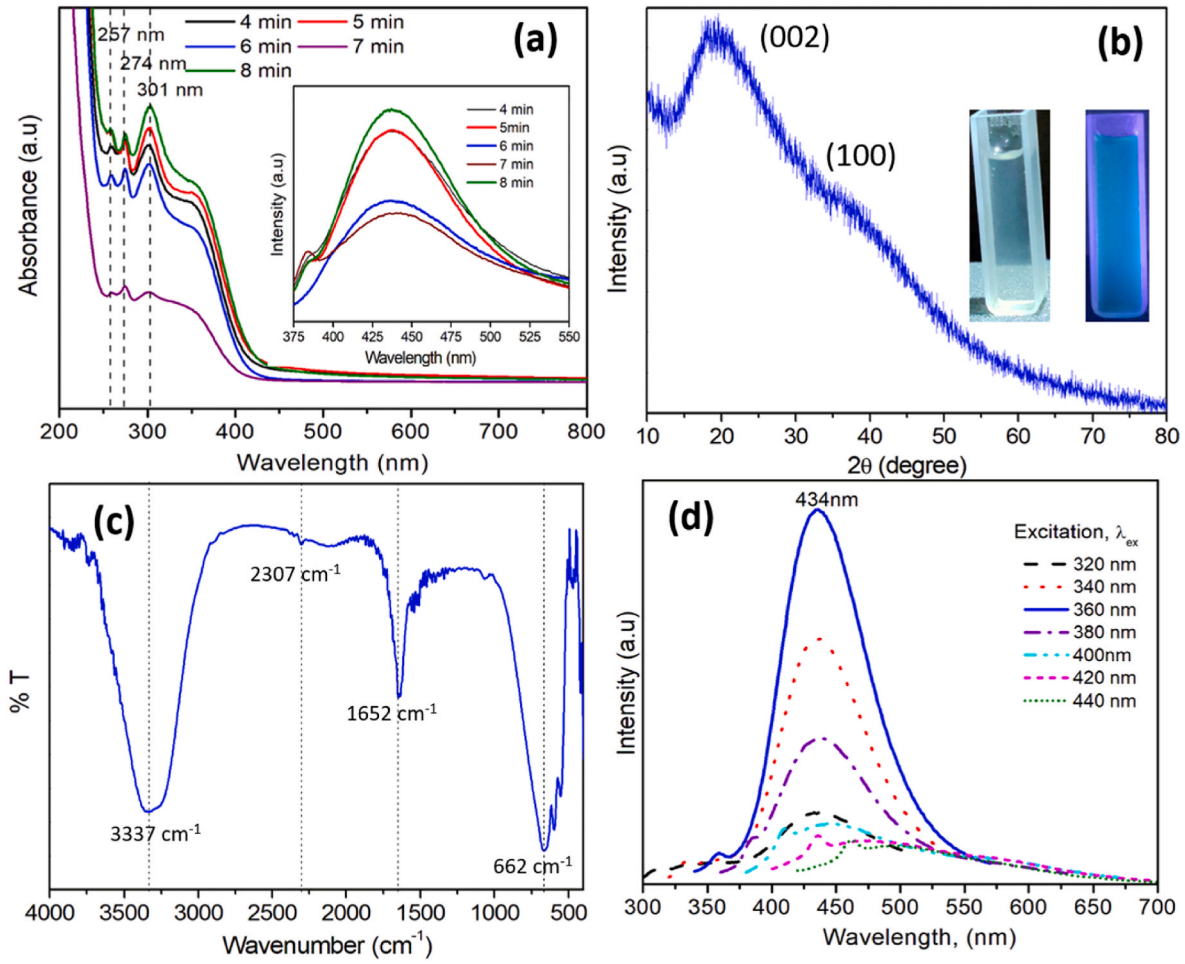

Fig. 2. (a) UV–Vis spectra of carbon quantum dots prepared from Aloe vera extract at various reaction periods (inset: The corresponding PL emission spectra of all CQDs excited at 360 nm), (b) XRD pattern, (c) FT-IR spectrum and (d) PL spectrum of CQDs prepared at 8 min.

3. Results and discussion

3.1. The formation mechanism of CQDs

Highly fluorescent carbon quantum dots are synthesized using the microwave-assisted reflux method directly from the Aloe vera extract without using any additional chemical reagents. The formation mechanism of CQDs by this method is coming under the category of the bottom-up approach. Few studies have reported the synthesis of CQDs by the microwave-assisted method using the biomass precursors of empty fruit bunch (Zaman et al., 2021), Mexican mint (Archita et al., 2021), *Gingko Biloba* (Genc et al., 2020), etc. However, the mechanism of CQD formation remains unclear since each precursor can contribute to different intermediate species (De Medeiros et al., 2019). In general, while irradiating the Aloe vera extract solution by applying thermal energy in terms of microwave power, the smaller carbon units (precursor molecules) converted into fluorophores. Upon continuous heating, the formed fluorophores undergo polymerization, condensation followed by carbonization that leads to the formation of CQDs (Ali et al., 2021).

3.2. UV–vis analysis

Fig. 2a shows the UV–visible spectra of CQDs prepared at different reaction periods of 4, 5, 6, 7 and 8 min. The peak observed in the UV region having maximum absorption at 301 nm with a tail extending to the visible region for all the samples. Besides, two small peaks arise before the maximum SPR peak at 257 nm and followed by 274 nm. The maximum absorption peak at 301 nm is due to the n-π* electronic transition of the C═O bond (Yang et al., 2020), and the other two small peaks are due to the π-π* electronic transition of the conjugated C═C bond (Ding et al., 2017; Han et al., 2017). The obtained maximum absorption (301 nm) is matched well with the reported CQDs (300 nm) prepared by the hydrothermal method using Chitosan as the raw materials (Yang et al., 2020). As well, both ginkgo (Zhang et al., 2019) and coriander leaves (Sachdev et al., 2015) derived CQDs provides the prominent absorption at 273 nm. On analyzing the effect of reaction time, it is found that CQDs synthesized at 8 min showed maximum absorbance in the UV–vis spectra (Fig. 2a) and also provides the maximum PL emission intensity at the excitation wavelength of 360 nm (Fig. 2a inset). Therefore, the CQDs prepared at 8 min was chosen for further studies.

3.3. XRD analysis

Fig. 2b represents the XRD pattern of carbon quantum dots prepared from Aloe vera extract. The XRD profiles of the synthesized CQDs having a broad diffraction peak centred around $2\theta = 20^{\circ}$ which can be attributed to the (002) lattice spacing of carbon-based materials with amorphous nature (Xu et al., 2020). The weak peak at $2\theta = 40^{\circ}$ can be assigned to the (100) diffraction pattern of synthesized CQDs (Chunduri et al., 2016), which confirms the amorphous nature. Similar XRD profile having $2\theta = 20^{\circ}$ was reported in the CQDs synthesized from walnut oil (Arkan et al., 2018) by hydrothermal method. The aqueous solution of

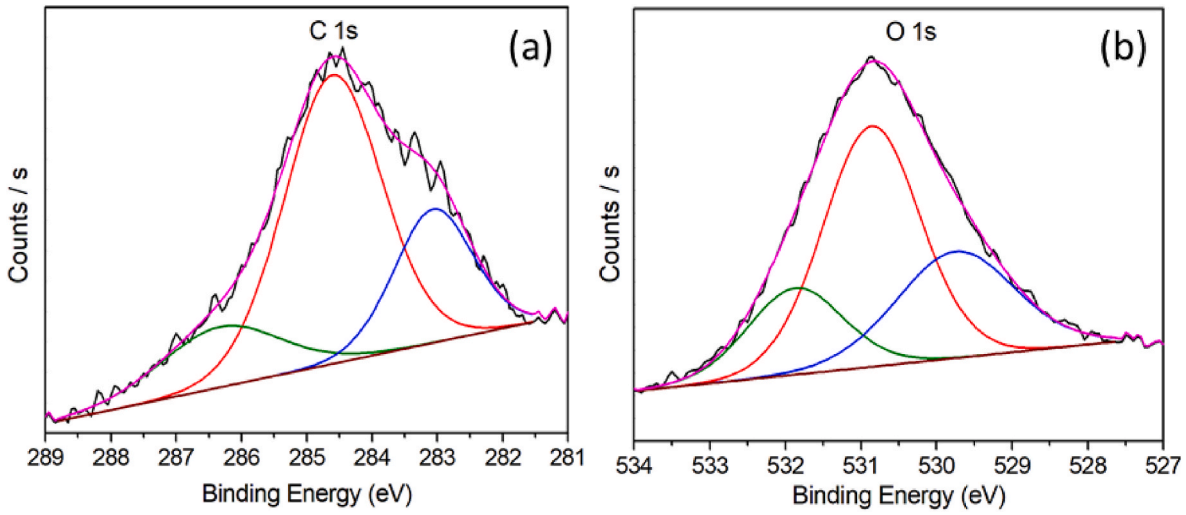

Fig. 3. The de-convoluted XPS spectra of (a) C 1s and (b) O 1s of CQDs.

CQDs appeared relatively transparent in daylight and it exhibited blue luminescence on the exposure of UV light (Fig. 2b inset).

3.4. FT-IR spectral analysis

The different bands observed in the FTIR spectrum (Fig. 2 c) infers the presence of certain functional groups located on the surface of CQDs. The observed broadband with a maximum at 3337 cm^{-1} and 1650 cm^{-1} denotes the presence of O–H and C═O groups in the CQDs (Boruah et al., 2020; Yan et al., 2020). The band observed at the fingerprint region of 662 cm^{-1} corresponds to the C–H bond (Zhu et al., 2020). Usually, the functional groups present on the surface can affect the optical properties of CQDs. In particular, the fluorescent properties of CQDs greatly depend upon the presence of various functional groups including OH, COOH, C═O, etc (Tang et al., 2019). Studies have also shown that the presence of carbonyl and hydroxyl groups contributes to the greater water-soluble nature of CQDs and helps in preventing post-synthetic aggregation without any surface passivation (Zhang et al., 2019; Jhonsi et al., 2018). It is worth mentioning that biomass precursors (Aloe vera) usually contains carbon and oxygen-rich compounds which might be the reason for the presence of carbonyl and hydroxyl groups on the synthesized CQDs.

3.5. PL analysis

Fig. 2d shows the PL spectra of CQDs at different excitation wavelengths from 320 to 420 nm. The emission peak at 434 nm with maximum intensity was obtained for the excitation wavelength of 360 nm. This blue emission of CQDs might have originated from the radiative combination of excited electrons from the n- π^* transition of the C═O groups (Hu et al., 2015). The literature depicts that the phenomena of exhibiting the blue fluorescence of CQDs are mainly due to the presence of the maximum amount of O–H groups (Das et al., 2019b). Especially, Du et al. (2016) have investigated the effect of functional groups on the visible fluorescence emission of GQDs and revealed that the O–H group has a major contribution to the emission of blue fluorescence. Further, while increasing the excitation wavelength from 360 to 420 nm, the emission intensity gets decreased. Usually, the excitation dependent emission wavelength significantly limits the application of CQDs because one has to use a series of different excitation sources to get different colours and the obtained long-wavelength emissions are usually very weak. But, the excitation independent wavelength emission can compensate for such deficiency (Wang et al., 2017a). Several reasons have been proposed to elucidate the wavelength independence of CQDs, such as the size distribution of carbon dots, the distribution of various emissive traps, the presence of oxygen-containing groups, pyrolytic development of various polyaromatic pyrophores within the carbogenic centre, free zig-zag sites and edge defects etc. (Chandra et al., 2013). The wavelength-independent behaviour could also be related to the presence of highly centralized particle size distribution (Wang et al., 2018). As well as the most important advantages of using the microwave-assisted reflux method are the synthesis of uniform-sized nanoparticles (Motshekga et al., 2012). Further, the CQD solutions have undergone centrifugation and dialysis, which altogether resulted in the presence of uniform, finite-sized, highly centred particles; hence there will be no wavelength dependency in the present case.

3.6. XPS analysis

The de-convoluted XPS spectra of CQDs (Fig. 3a,b) shows two narrow and strong peaks at 284.6 eV and 531.61eV corresponding to C 1s and O 1s, respectively. It indicates that the synthesized CQDs contain mainly carbon and oxygen, having an atomic percentage of 56.33% and 43.67%, respectively. The high-resolution C1s peak is de-convoluted into three distinct peaks at 284.6 eV, 286.33 eV and 283.06 eV, confirming the presence of functional groups like C═C, C═O and C–C (Dager et al., 2019; Far'ain et al., 2017; Wu et al., 2015), respectively. On de-convolution of O 1s spectrum, three peaks are observed in which peaks at 530.86 eV and 529.75 eV indicates the presence of C═O groups, whereas the peak at 531.87 eV can be attributed to the presence of C–OH/C–O–C groups (Guo et al., 2017; Zhao et al., 2019). As there is no significant trace of any other residual elements, which indicate the purity of the prepared CQDs.

3.7. Quantum yield

The quantum yield can measure the efficiency of the fluorescence property of CQDs. Quantum yield is described as the efficiency of conversion of absorbed light into emitted light, in the form of fluorescence. It is a measure of photon emission efficiency, by determining the ratio of the number of the emitted photons to the number of absorbed photons. The QY of the CQDs is determined with quinine sulphate as standard. The relative QY of Aloe vera derived CQDs is 31%, which is much higher than the QY of 10.37%, and 16.4% of Aloe vera derived CQDs, from hydrothermal (Xu et al., 2015) and carbonization method (Sarkar et al., 2017), respectively. The hydroxyl groups on the surface of CQDs may contribute to high fluorescent quantum yield (Xu et al., 2015).

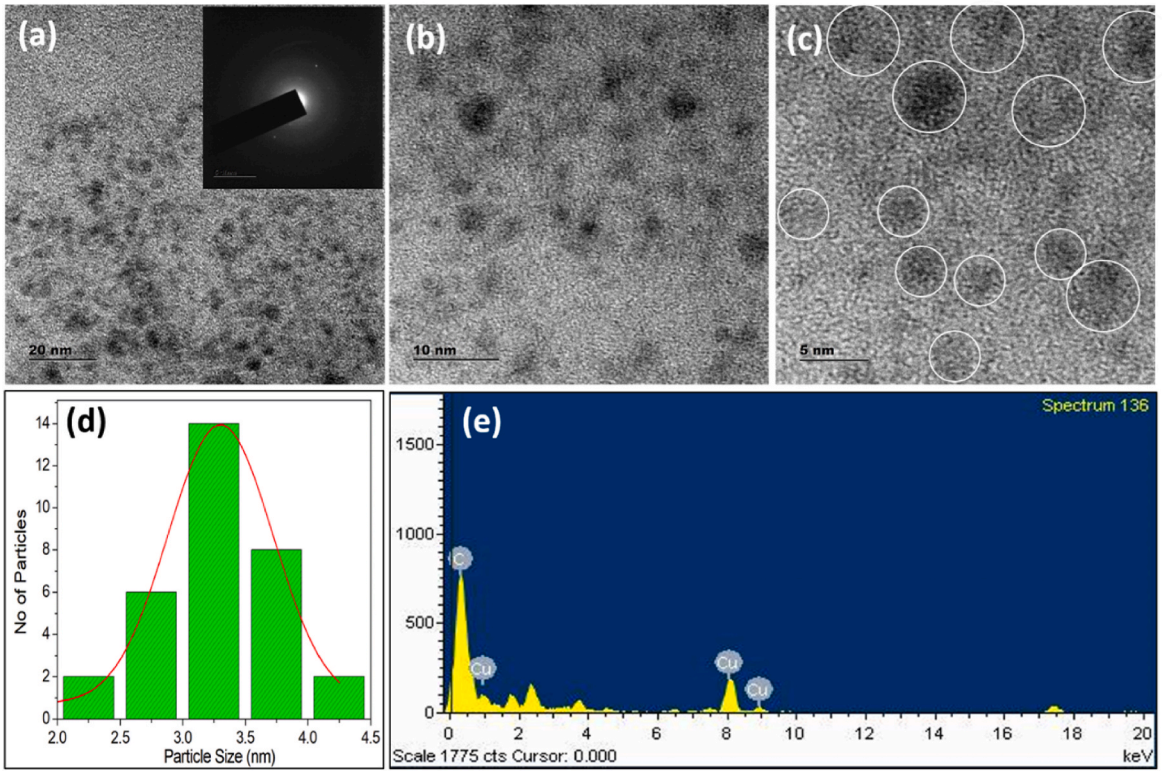

Fig. 4. (a–c) HRTEM image of CQDs prepared from Aloe vera extract, (d) Particle size histogram and (e) EDAX analysis.

3.8. TEM and HRTEM analysis

Fig. 4(a–c) shows the HRTEM images of the synthesized CQDs. It infers that the particles are spherical, monodisperse and without any aggregation. The observed size of the particles is less than 5 nm. The particle size histogram (Fig. 4d) elucidates that the CQDs have a narrow size distribution centring around 3–3.5 nm, with an average size of 3.2 nm. The SAED pattern further confirms that the synthesized CQDs are amorphous in nature (Fig. 4a inset). EDX analysis was performed to investigate the elemental analysis of synthesized CQDs, as shown in Fig. 4e, which reveals the samples containing the maximum amount of carbon. This can be attributed to the presence of carbon-containing (Organic) compounds in Aloe vera leaf (Banik et al., 2019).

3.9. Photocatalytic degradation studies of eosin yellow

The degradation efficiency of the prepared CQDs was analyzed by using the anionic dye, EY in an aqueous solution without the combination of any semiconductor nanomaterial or heteroatom doping. Fig. 5a shows the UV–vis absorption spectra of the EY in the presence of CQDs measured at a regular interval of 20 min with the characteristic wavelength of 517 nm. It is observed that the gradual decrease and final disappearance of the characteristic absorption peak (at 517 nm) from 0 to 120 min. The temporal concentration changes (C/C_o) of EY indicates a steady decrease of the dye concentration with time, with a photodegradation efficiency of 98.55% within 80 min (Fig. 5b and inset). The solution becomes colourless after 100 min thereby achieving an efficiency of 100% and hence indicating complete degradation of the dye in the aqueous solution. It shows that the removal rate of dye increases as the contact time increases and the absorbance decreases until the absorption rate reached the equilibrium for adsorbent after 80 min.

The reaction rate in the photodegradation experiment was determined using pseudo-first-order kinetics: $\ln(C_o/C) = kt$, where C_o is the initial concentration of EY before illumination and C is the concentration of EY with respect to time t, k is the reaction rate, and t is the reaction time during EY decomposition. The reaction rate (k) of the photodecomposition of EY was estimated by drawing a graph between ln (C_o/C) and t (Fig. 5b inset). It reveals that the photocatalytic degradation is utterly consistent with the pseudo-first-order kinetics, with a degradation rate constants of 2.079×10^{-2} min^{-1}. The photocatalytic degradation performances of the present work are comparable to other carbon-based NP's especially graphene-based nanostructures (Ojha et al., 2020) and graphite nanocomposite (Ndlovu et al., 2014) for EY degradation.

The high photodegradation efficiency obtained by the CQDs can be attributed to the adsorption of EY dye molecules by CQDs. There are different adsorption mechanisms such as hydrogen bonding, electrostatic and π- π* interactions etc., for the adsorption of dyes into photocatalysts surface (Veerakumar et al., 2017). As well as the photocatalytic efficiency of CQDs is strongly dependent on the surface chemistry and surface functionalization of CQDs for the effective separation of charge carriers (Phang et al., 2019). However, very few studies have depicted the use of pure CQDs as photocatalysts for the degradation of organic dyes and revealed that the photodegradation was predominantly attributed by the surface states (Pirsaheb et al., 2018; Sabet et al., 2019). The FTIR and XPS analysis infer that the presence of abundant hydroxyl as well as oxygen-containing functional groups on the CQDs. These oxygen-containing functional groups and delocalized π electrons can effectively interact with the EY dye molecule. Similarly, the C═C and C—H stretching bands create a strong π- π* interaction between the delocalized π electron of aromatic rings of CQDs and EY. A similar type of observations has been reported by Veerakumar et al. (2017) for the photodegradation of EY using graphene oxide nanosheets. The mechanism for photocatalytic degradation of organic dyes by carbon dots was proposed by Peng et al. (2020). The high photocatalytic efficiency of CQDs can be attributed to their visible light absorption capacity and abundance of optically active centres.

Fig. 5c explains the plausible degradation mechanism of EY by CQDs. As CQDs were excited by photons of sufficient energy, electrons were excited from the ground state to the excitation state, generating excess

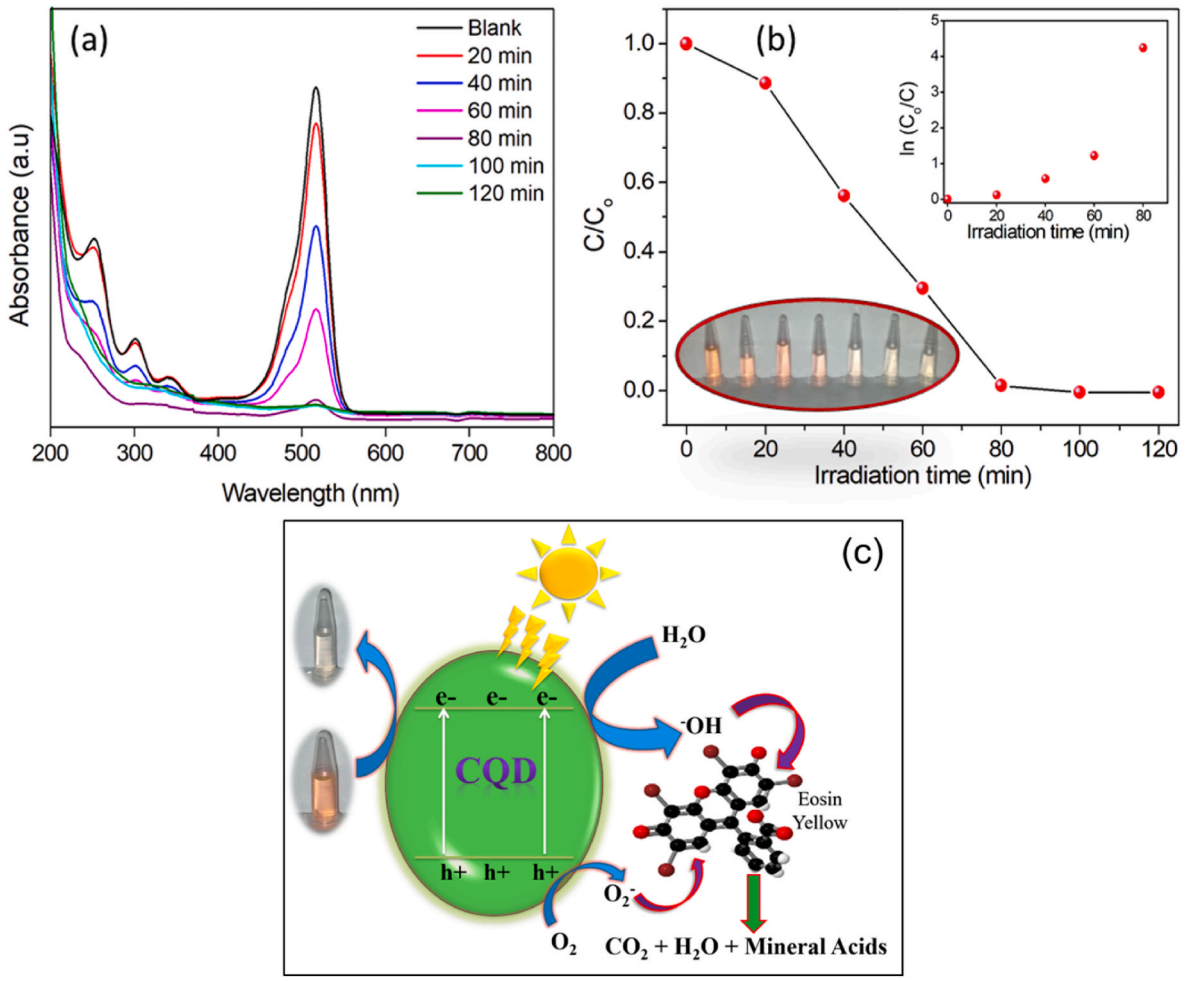

Fig. 5. (a) UV–visible absorption spectra elucidating the photocatalytic activity of CQDs towards the photocatalytic degradation of Eosin Yellow, (b) Kinetics of EY degradation (inset: the photographic image of EY solution at different time periods) and (c) Tentative scheme for the degradation mechanism. (For interpretation of the references to colour in this figure legend, the reader is referred to the Web version of this article.)

electrons (e^-) and holes (h^+). Owing to the rich nature of surface defects (i.e. surface functionalities) on CQDs, some of the excited carriers are trapped, and the recombination of e^- and h^+ is inhibited. As a result, organic dyes could be oxidized directly by h^+ to induce degradation. Some of the h^+ could interact with surface-adsorbed H_2O to generate hydroxyl radicals (i.e., $^{\cdot}OH$). Occasionally, some of the e^- could be absorbed by oxygen dissolved in solution, creating superoxide radicals also (i.e., $^{\cdot}O^{2-}$) (Das et al., 2019a). The produced reactive oxygen species (ROS) reacts with the EY molecule and releases the CO_2, H_2O and mineral acids as by-products (Rani Rosaline et al., 2020). Further, the surface hydroxyl groups (OH) on the surface of CQDs could act as the active sites for the photocatalytic reactions by effective H-bonding interactions with dye molecules (Das et al., 2019a). However further studies will be needed to quantify the specific performance of ROS and reveal the exact degradation pathway of EY. Nevertheless, considering the excellent photocatalytic activity of CQDs towards the degradation of EY, as well as the fact that they are easily synthesized without the need for further doping, compositing, and time-consuming purification and separation, the CQDs developed in this work are shown to be a promising alternative for environmental remediation.

3.10. MTT assay

The cell viability and the possible apoptosis effect of CQDs were evaluated using the MTT assay on the MCF-7 human breast cancer cell line. Cancerous breast cells had diverse concentrations ranges from 0 to 100 μg/mL in CQDs for 24 h, as found in Fig. 6, demonstrating a notable reduction in cell viability in a dose-subjected manner. The synthesized CQDs induced 50% (IC_{50}) of inhibition activity against MCF 7 cells at a

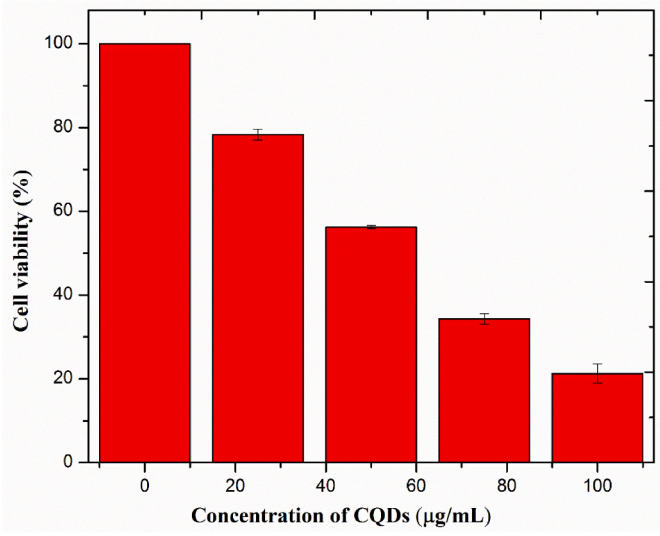

Fig. 6. MTT assay of CQDs in MCF-7 human breast cancer cell line.

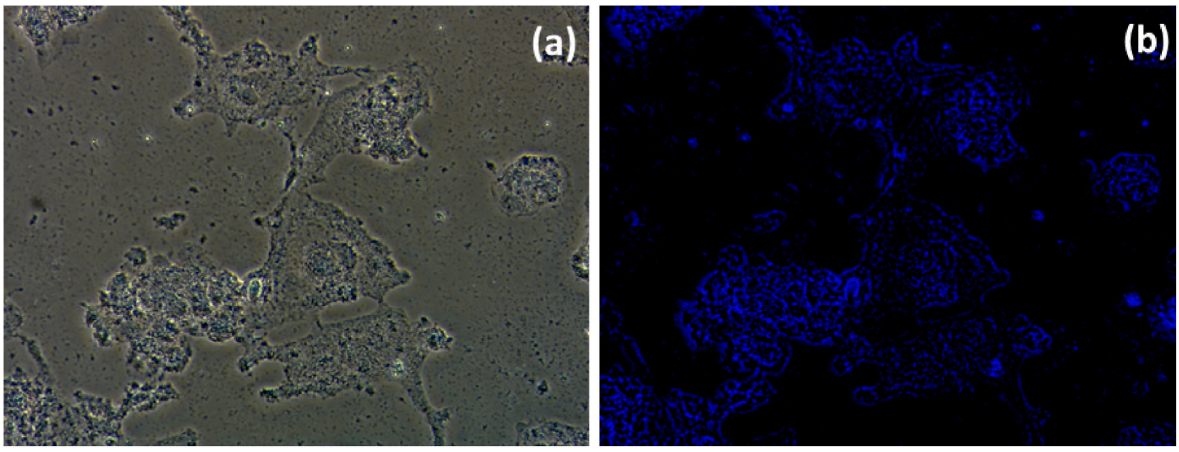

Fig. 7. Confocal fluorescence microscopic images of CQDs labelled MCF-7 cells (a) under bright field (b) UV light excitation.

concentration of 52.2 ± 1.35 μg/mL, thereby clearly demonstrating the anti-proliferative and apoptosis effect of CQDs in human breast cancer cells. A similar finding was reported by Basak et al. (2017), who revealed that Aloe vera whole leaf extract has the potential to inhibit the growth of MCF 7 breast cancer cell. The literature depicts that Aloe vera has the anticancer property since it is containing aloe-emodin, aloin (barbaloin), anthracene and emodin compounds, as well as phytochemicals including alkaloids, phenols, and flavonoids (Rahmani et al., 2015; Basak et al., 2017). Therefore, the synthesized CQDs derived from Aloe vera also having better cytotoxicity properties.

3.11. Bio-imaging analysis

In recent years, bio-imaging is a method for direct visualization of biological processes in real-time, and this can act as an effective method for the diagnosis of cancer cells. The bioimaging potential of as-prepared CQDs was tested by treating MCF-7 human breast cancer cell lines with 10 μL of CQDs derived from Aloe vera extract. Cell images were recorded with fluorescence microscopy under a blue filter. Fig. 7a shows the phase-contrast microscopic images of the MCF-7 cell line after incubation with CQDs. Upon uptake, the cells were found to be normal and found less toxic at (10 μL). Meanwhile, Fig. 7b shows the bright blue luminescence within the cells inferring the rapid internalization and excellent permeability of CQDs. The FT-IR and XPS results revealed that the surface of CQDs contains hydroxyl and carbonyl groups. From the study conducted by Zhang et al. (2019), the presence of hydrophilic –OH groups and the presence of C═O groups (Jhonsi et al., 2018) was beneficial for biological imaging (Dong et al., 2018). Therefore, the results indicate that the CQDs derived from Aloe vera can be used as an excellent biomarker or bioimaging probe. Similarly, CQDs synthesized from *Catharanthus roseus* by the hydrothermal method also showed bright fluorescence emission on MCF 7 cell lines (Arumugham et al., 2020). CQDs synthesized from *Allium fistulosum* by hydrothermal method exhibited blue fluorescence in MCF 7 cells when excited at 405 nm (Wei et al., 2019) and those synthesized from seeds, leaves, and cysteine of tobacco by mixed acid oxidation emitted blue fluorescence at 400 nm excitation (Dong et al., 2018). In the present work, Aloe vera derived CQDs exhibited both bioimaging as well as anticancer properties and acted as multifunctional biomedical nanoagent which can diagnose cancer and inhibit it by cytotoxic activity and are expected to have great potential in future clinical applications.

4. Conclusions

In this article, we have demonstrated a facile method to prepare bright blue-emitting carbon quantum dots from Aloe vera leaf using the microwave-assisted reflux method within a concise duration of 8 min. The prepared CQDs are spherical, monodispersed with narrow size distribution having less than 5 nm size. XRD analysis revealed that the synthesized carbon quantum dots are amorphous. Their aqueous solutions emitted bright blue light under UV irradiation, indicating the photoluminescence property. Excitation independent emission wavelength was observed, which arise due to the uniform size of particles (monodispersity) as a result of the microwave-assisted reflux method. FT-IR analysis demonstrates the carbon quantum dots contains hydroxyl and carbonyl groups, which is responsible for luminescence making them applicable in bio labelling and bioimaging. It also helps carbon quantum dots to disperse in an aqueous solution uniformly. The CQDs showed excellent photocatalytic activity by degrading eosin yellow dye under solar light irradiation, leading to complete degradation within 100 min. Effect of CQDs on cell viability of MCF-7 human breast cancer cell line analyzed using MTT assay revealed the potential apoptosis effect of CQDs in human breast cancer cell line, in a dose-dependent manner. Further, CQDs can be an excellent fluorescent agent that gets internalized by the cells for live-cell bio-imaging studies. Therefore, these multifunctional CQDs which could exhibit bioimaging, anticancer and photocatalytic applications may be considered as an economical and easily accessible source of effective agents used in cancer therapy paving a path for its potential applications in better cancer treatments as well as for remediation of organic dye pollutants in aqueous media.

Credit author statement

Jalaja Prasad Malavika: Investigation, Writing - Original Draft, **Chellappan Shobana:** Conceptualization, Methodology, Supervision, **Murugesan Ragupathi:** Investigation, **Ponnuchamy Kumar:** Resources,**Yun Sung Lee:** Resources,**Muthusamy Govarthanan:** Resources, **Ramakrishnan Kalai Selvan:** Conceptualization, Methodology, Supervision

Funding

Prof. Yun Sung Lee gratefully acknowledge the financial support from the National Research Foundation of Korea (NRF) grant funded by the Korean government (Ministry of Science, ICT & Future Planning) (No. 2019R1A4A2001527).

Declaration of competing interest

The authors declare that they have no known competing financial interests or personal relationships that could have appeared to influence the work reported in this paper.

Acknowledgement

The authors, Ms J.P.Malavika and Dr C.Shobana would like to thank the Management of Kongunadu Arts and Science College, Coimbatore, for their valuable support and encouragement.

References

Alam, A.M., Park, B.Y., Ghouri, Z.K., Park, M., Kim, H.Y., 2015. Synthesis of carbon quantum dots from cabbage with down- and up-conversion photoluminescence properties: excellent imaging agent for biomedical applications. Green Chem. 17, 3791–3797.

Ali, M., Riaz, R., Anjum, A.S., Sun, K.C., Li, H., Ahn, S., Jeong, S.H., Ko, M.J., 2021. Microwave-assisted ultrafast in-situ growth of N-doped carbon quantum dots on multiwalled carbon nanotubes as an efficient electrocatalyst for photovoltaics. J. Colloid Interface Sci. 585, 349–361.

Anirudhan, T.S., Rejeena, S.R., 2015. Photocatalytic degradation of eosin yellow using poly(pyrrole-co-aniline)-coated TiO_2/nanocellulose composite under solar light irradiation. J. Mater. 2015, 636409.

Architha, N., Ragupathi, M., Shobana, C., Selvankumar, T., Kumar, P., Lee, Y.S., Selvan, R.K., 2021. Microwave-assisted green synthesis of fluorescent carbon quantum dots from Mexican Mint extract for Fe^{3+} detection and bio-imaging applications. Environ. Res. 199, 111263.

Arkan, E., Barati, A., Rahmanpanah, M., Hosseinzadeh, L., Moradi, S., Hajialyani, M., 2018. Green synthesis of carbon dots derived from walnut oil and an investigation of their cytotoxic and apoptogenic activities toward cancer cells. Adv. Pharmaceut. Bull. 8, 149–155.

Arumugham, T., Alagumuthu, M., Amimodu, R.G., Munusamy, S., Iyer, S.K., 2020. A sustainable synthesis of green carbon quantum dot (CQD) from *Catharanthus roseus* (white flowering plant) leaves and investigation of its dual fluorescence responsive behavior in multi-ion detection and biological applications. Sustainable Materials and Technologies 23, e00138.

Banik, S., Sharangi, A.B., 2019. Phytochemistry, health benefits and toxicological profile of aloe. J. Pharmacogn. Phytochem. 8, 4499–4506.

Basak, P., Paul, S., Majumder, R., 2017. Invitro cytotoxic study of Aloe vera whole leaf Extract on PBMC and breast cancer cell line. In: 2nd International Conference for Convergence in Technology, I2CT, pp. 124–127.

Boruah, A., Saikia, M., Das, T., Goswamee, R.L., Saikia, B.K., 2020. Blue-emitting fluorescent carbon quantum dots from waste biomass sources and their application in fluoride ion detection in water. J. Photochem. Photobiol., B 209, 111940.

Chandra, S., Patra, P., Pathan, S.H., Roy, S., Mitra, S., Layek, A., Bhar, R., Pramanik, P., Goswami, A., 2013. Luminescent S-doped carbon dots: an emergent architecture for multimodal applications. J. Mater. Chem. B 1, 2375–2382.

Chunduri, L.A.A., Avinash Chunduri, L.A., Kurdekar, A., Patnaik, S., Vishnu, D.B., Mimani, R.T., Kamisetti, V., 2016. Carbon quantum dots from coconut husk: evaluation for antioxidant and cytotoxic activity. Materials Focus 5, 55–61.

Dager, A., Uchida, T., Maekawa, T., Tachibana, M., 2019. Synthesis and characterization of monodisperse carbon quantum dots from fennel seeds: photoluminescence analysis using machine learning. Sci. Rep. 9, 14004.

Das, G.S., Shim, J.P., Bhatnagar, A., Tripathi, K.M., Kim, T.Y., 2019a. Biomass-derived carbon quantum dots for visible-light-induced photocatalysis and label-free detection of Fe(III) and ascorbic acid. Sci. Rep. 9, 15084.

Das, T., Saikia, B.K., Dekaboruah, H.P., Bordoloi, M., Neog, D., Bora, J.J., Lahkar, J., Narzary, B., Roy, S., Ramaiah, D., 2019b. Blue-fluorescent and biocompatible carbon dots derived from abundant low-quality coals. J. Photochem. Photobiol., B 195, 1–11.

De Medeiros, T.V., Tayline, V., Manioudakis, J., 2019. Microwave-assisted synthesis of carbon dots and their applications. J. Mater. Chem. C. 7, 7175–7195.

Ding, Y., Zhang, F., Xu, J., Miao, Y., Yang, Y., Liu, X., Xu, B., 2017. Synthesis of short-chain passivated carbon quantum dots as the light emitting layer towards electroluminescence. RSC Adv. 7, 28754–28762.

Dong, L., Liu, D., Li, X., Wu, Zhang, W., 2018. Synthesis and characterization of biomass CQDs doped $WO_{2.72}$. Results in Physics 11, 482–488.

Du, J., Wang, H., Wang, L., Zhu, S., Song, Y., Yang, B., Sun, H., 2016. Insight into the effect of functional groups on visible-fluorescence emissions of graphene quantum dots. J. Mater. Chem. C 4, 2235–2242.

Far'ain, N., Salleh, M.M., Ashraf, M., Abd Rahman, M.Y., Umar, A.A., 2017. Synthesis of blue-luminescence graphene quantum dots using hydrothermal method. Solid State Phenom. 268, 259–263.

Genc, M.T., Yanalak, G., Arslan, G., Patir, I.H., 2020. Green preparation of carbon quantum dots using *Gingko biloba* to sensitize TiO_2 for the photohydrogen production. Mater. Sci. Semicond. Process. 109, 104945.

Guo, Y., Chen, Y., Cao, F., Wang, L., Wang, Z., Leng, Y., 2017. Hydrothermal synthesis of nitrogen and boron doped carbon quantum dots with yellow-green emission for sensing Cr(vi), anti-counterfeiting and cell imaging. RSC Adv. 7, 48386–48393.

Han, B., Yu, M., Pen, T., Li, Y., Hu, X., Xiang, R., Hou, X., He, G., 2017. One-step extraction of highly fluorescent carbon quantum dots by a physical method from carbon black. New J. Chem. 41, 5267–5270.

Hasan, M., Saha, R., Quaid, N., Reza, M.T., 2021. Formation of carbon quantum dots via hydrothermal carbonization: investigate the effect of precursors. Energies 14, 986.

Hu, S., Trinchi, A., Atkin, P., Cole, I., 2015. Tunable photoluminescence across the entire visible spectrum from carbon dots excited by white light. Angew. Chem. Int. Ed. 54, 2970–2974.

Hussain, A., Sharma, C., Khan, S., Shah, K., Haque, S., 2015. Aloe vera inhibits proliferation of human breast and cervical cancer cells and acts synergistically with cisplatin. Asian Pac. J. Cancer Prev. APJCP 16, 2939–2946.

Jhonsi, M.A., 2018. Carbon quantum dots for bioimaging, state of the art in nano-bioimaging. In: Ghamsari, Morteza Sasani (Ed.), IntechOpen. https://doi.org/10.5772/intechopen.72723.

Karthik, R., Muthezhilan, R., Jaffar Hussain, A., Ramalingam, K., Rekha, V., 2016. Effective removal of methylene blue dye from water using three different low-cost adsorbents. Desalination Water Treat 57, 10626–10631.

Li, C.L., Ou, C.M., Huang, C.C., Wu, W.C., Chen, Y.P., Lin, T.E., Ho, L.C., Wang, C.W., Shih, C.C., Zhou, H.C., Lee, Y.C., Tzeng, W.F., Chiou, T.J., Chu, S.T., Cang, J., Chang, H.T., 2014. Carbon dots prepared from ginger exhibiting efficient inhibition of human hepatocellular carcinoma cells. J. Mater. Chem. B 2, 4564–4571.

Majek, M., Filace, F., Wangelin, A.J., 2014. On the mechanism of photocatalytic reactions with eosin Y. Beilstein J. Org. Chem. 10, 981–989.

Mittal, A., Jhare, D., Mittal, J., 2013. Adsorption of hazardous dye eosin yellow from aqueous solution onto waste material De-oiled Soya: isotherm, kinetics and bulk removal. J. Mol. Liq. 179, 133–140.

Molaei, M.J., 2019. Carbon quantum dots and their biomedical and therapeutic applications: a review. RSC Adv. 9, 6460–6481.

Motshekga, S.C., Pillai, S.K., Ray, S.S., Jalama, K., Krause, R.W.M., 2012. Recent trends in the microwave assisted synthesis of metal oxide nanoparticles supported on carbon nanotubes and their applications. J. Nanomater. 2012, 691503.

Nandal, U., Bhardwaj, R.L., 2012. Aloe vera: a valuable wonder plant for food, medicine and cosmetic use - a review. Int. J. Pharmaceut. Sci. Rev. Res. 13, 59–67.

Ndlovu, T., Kuvarega, A.T., Arotiba, O.A., Sampath, S., Krause, R.W., Mamba, B.B., 2014. Exfoliated graphite/titanium dioxide nanocomposites for photodegradation of eosin yellow. Appl. Surf. Sci. 300, 159–164.

Ojha, A., Thareja, P., 2020. Graphene-based nanostructures for enhanced photocatalytic degradation of industrial dyes. Emergent Materials 3, 169–180.

Peng, Z., Zhou, Y., Ji, C., Pardo, J., Mintz, K.J., Pandey, R.R., Chusuei, C.C., Graham, R. M., Yan, G., Leblanc, R.M., 2020. Facile Synthesis of "Boron-Doped" carbon dots and their application in visible-light-driven photocatalytic degradation of organic dyes. Nanomaterials 10, 1560.

Phang, S.J., Tan, L.L., 2019. Recent advances in carbon quantum dot (CQD)-based two dimensional materials for photocatalytic applications. Catal. Sci. Technol. 9, 5882–5905.

Pirsaheb, M., Asadi, A., Sillanpää, M., Farhadian, N., 2018. Application of carbon quantum dots to increase the activity of conventional photocatalysts: a systematic review. J. Mol. Liq. 271, 857–871.

Rahmani, A.H., Aldebasi, Y.H., Srikar, S., Khan, A.A., Aly, S.M., 2015. Aloe vera: potential candidate in health management via modulation of biological activities. Pharm. Rev. 9, 120–126.

Rani Rosaline, D., Inbanathan, S.S.R., Suganthi, A., Rajarajan, M., Kavitha, G., Srinivasan, R., Hegazy, H.H., Umar, A., Algarni, H., Manikandan, E., 2020. Visible-light driven photocatalytic degradation of eosin yellow (EY) dye based on NiO-WO_3 nanoparticles. J. Nanosci. Nanotechnol. 20, 924–933.

Sabet, M., Mahdavi, K., 2019. Green synthesis of high photoluminescence nitrogen-doped carbon quantum dots from grass via a simple hydrothermal method for removing organic and inorganic water pollution. Appl. Surf. Sci. 463, 283–291.

Sachdev, A., Gopinath, P., 2015. Green synthesis of multifunctional carbon dots from coriander leaves and their potential application as antioxidants, sensors and bioimaging agents. Analyst 140, 4260–4269.

Sagbas, S., Sahiner, N., 2019. Carbon dots: preparation, properties, and application. In: Khan, Anish, Jawaid, Mohammad, Inamuddin, Asiri, Abdullah mohamed (Eds.), Woodhead Publishing Series in Composites Science and Engineering, Nanocarbon and its Composites. Woodhead Publishing, ISBN 9780081025093, pp. 651–676.

Sarkar, N., Sahoo, G., Das, R., Prusty, G., Swain, S.K., 2017. Carbon quantum dot tailored calcium alginate hydrogel for pH responsive controlled delivery of vancomycin. Eur. J. Pharmaceut. Sci. 109, 359–371.

Semeniuk, M., Yi, Z., Poursorkhabi, V., Tjong, J., Jaffer, S., Lu, Z.H., Sain, M., 2019. Future perspectives and review on organic carbon dots in electronic applications. ACS Nano 13, 6224–6255.

Shalabi, M., Khilo, K., Zakaria, M.M., Elsebaei, M.G., Abdo, W., Awadin, W., 2015. Anticancer activity of Aloe vera and *Calligonum comosum* extracts separately on hepatocellular carcinoma cells. Asian Pac. J. Trop. Biomed. 5, 375–381.

Shobana, C., Rangasamy, B., Surendran, S., Selvan, R.K., Ramesh, M., 2018. Green synthesized silver nanoparticles and their impact on the antioxidant response and histology of Indian major carp *Labeo rohita*, with combined response surface methodology analysis. J. Cluster Sci. 29, 267–279.

Singh, J., Dutta, T., Kim, K.H., Mohit, R., Samddar, P., Kumar, P., 2018. "Green" synthesis of metals and their oxide nanoparticles: applications for environmental remediation. J. Nanobiotechnol. 16, 84.

Singh, R.K., Kumar, R., Singh, D.P., Savu, R., Moshkalev, S.A., 2019. Progress in microwave-assisted synthesis of quantum dots (graphene/carbon/semiconducting) for bioapplications: a review. Materials Today Chemistry 12, 282–314.

Tang, J., Zhang, J., Zhang, Y., Xiao, Y., Shi, Y., Chen, Y., Ding, L., Xu, W., 2019. Influence of group modification at the edges of carbon quantum dots on fluorescent emission. Nanoscale Res. Lett. 14, 241.

Veerakumar, P., Tharini, J., Ramakrishnan, M., Muthuselvam, I.P., Lin, K.C., 2017. Graphene oxide nanosheets as an efficient and reusable sorbents for eosin yellow dye removal from aqueous solutions. ChemistrySelect 2, 3598–3607.

Wang, R., Lu, K-Q., Tang, Z-R., Xu, Y-J., 2017b. Recent progress in carbon quantum dots: synthesis, properties and applications in photocatalysis. J. Mater. Chem. A 5, 3717–3734.

Wang, H., Ning, G., He, X., Ma, X., Yang, F., Xu, Z., Zhao, S., Xu, C., Li, Y., 2018. Carbon quantum dots derived by direct carbonization of carbonaceous microcrystals in mesophase pitch. Nanoscale 10, 21492–21498.
Wang, X., Feng, Y., Dong, P., Huang, J., 2019. A mini review on carbon quantum dots: preparation, properties, and electrocatalytic application. Front. Chem. 7, 671.
Wang, H., Sun, C., Chen, X., Zhang, Y., Colvin, V.L., Rice, Q., Seo, J., Feng, S., Wang, S., Yu, W.W., 2017a. Excitation wavelength independent visible color emission of carbon dots. Nanoscale 9, 1909–1915.
Wei, Z., Wang, B., Liu, Y., Liu, Z., Zhang, H., Zhang, S., Chang, J., Lu, S., 2019. Green synthesis of nitrogen and sulfur co-doped carbon dots from Allium fistulosum for cell imaging. New J. Chem. 43, 718–723.
Wu, W., Zhan, L., Ohkubo, K., Yamada, Y., Wu, M., Fukuzumi, S., 2015. Photocatalytic H_2 evolution from NADH with carbon quantum dots/Pt and 2-phenyl-4-(1-naphthyl) quinolinium ion. J. Photochem. Photobiol. B: Biol. 152, 63–70.
Xu, H., Yang, X., Li, G., Zhao, C., Liao, X., 2015. Green synthesis of fluorescent carbon dots for selective detection of Tartrazine in food samples. J. Agric. Food Chem. 63, 6707–6714.
Xu, J., Wang, C., Li, H., Zhao, W., 2020. Synthesis of green-emitting carbon quantum dots with double carbon sources and their application as a fluorescent probe for selective detection of Cu^{2+} ions. RSC Adv. 10, 2536–2544.
Yan, C., Ren, Y., Sun, X., Jin, L., Liu, X., Chen, H., Wang, K., Yu, M., Zhao, Y., 2020. Photoluminescent functionalized carbon quantum dots loaded electroactive Silk fibroin/PLA nanofibrous bioactive scaffolds for cardiac tissue engineering. J. Photochem. Photobiol., B 202, 111680.
Yang, Q., Yang, W., Zhang, Y., Ge, W., Yang, X., Yang, P., 2020. Precise surface state control of carbon quantum dots to enhance charge extraction for solar cells. Nanomaterials 10, 460.
Yao, H., Li, J., Song, Y., Zhao, H., Wei, Z., Li, X., Jin, Y., Yang, B., Jiang, J., 2018. Synthesis of ginsenoside Re-based carbon dots applied for bioimaging and effective inhibition of cancer cells. Int. J. Nanomed. 13, 6249–6264.
Zaman, A.S.K., Tan, T.L., Chowmasundaram, Y., Jamaludin, N., Sadrolhosseini, A.R., Rashid, U., Rashid, S.A., 2021. Properties and molecular structure of carbon quantum dots derived from empty fruit bunch biochar using a facile microwave-assisted method for the detection of Cu^{2+} ions. Opt. Mater. 112, 110801.
Zhang, Q., Zhang, X., Bao, L., Wu, Y., Jiang, L., Zheng, Y., Wang, Y., Chen, Y., 2019. The application of green-synthesis-derived carbon quantum dots to bioimaging and the Analysis of Mercury (II). J Anal Methods Chem 2019, 8183134.
Zhao, J., Song, Q., Wu, F., Guo, X., Xu, T., 2019. Green synthesis of N-doped carbon quantum dots for the detection of nitrite ion in water sample. IOP Conf. Ser. Earth Environ. Sci. 344, 012068.
Zheng, H., Pan, Y., Xiang, X., 2007. Oxidation of acidic dye Eosin Y by the solar photo-Fenton processes. J. Hazard Mater. 141, 457–464.
Zhu, J., Chu, H., Wang, T., Wang, C., Wei, Y., 2020. Fluorescent probe based nitrogen dopedcarbon quantum dots with solid-state fluorescence for the detection of Hg^{2+} and Fe^{3+} in aqueous solution. Microchem. J. 158, 105142.